

A Highschooler's Guide to GeV-Range Electromagnetism

Satchit Chatterji, Aayush Desai, Aditya Dwarkesh,
Anushree Ganesh, Ameya Kunder, Pulkit Malhotra,
Roshni Sahoo, Jinal Shah and Kiranbhaskar Velmurugan
*R.N. Podar School (CBSE), Jain Derasar Marg,
Santacruz West Mumbai – 400054, Maharashtra, India
cryptic.ontics@gmail.com*

Markus Joos and Cristóvão Beirão Da Cruz E Silva
*CERN, Espl. des Particules 1,
1211 Meyrin, Switzerland*

Gianfranco Morello
*Laboratori Nazionali di Frascati dell'INFN,
via E. Fermi 54, 00044 Frascati, Italy*

Received August 14, 2020

The following article has been written primarily by the high school students who make up the team “Cryptic Optics”, one of the two winning teams in the 2018 edition of CERN’s Beamline for Schools (BL4S) competition, and is based on the set of experiments the students endeavoured to conduct over the course of a two-week period at CERN.

Reconstructing influential physical theories from scratch often helps in uncovering hitherto unknown logical connections and eliciting instructive empirical checkpoints within said theory. With this in mind, in the following article, a top-down reconstruction (beginning with the experimental observations and ending at the theoretical framework) of the Lorentz force equation is performed, and potentially interesting questions which come up are explored. In its most common form, the equation is written out as: $\mathbf{F} = q\mathbf{E} + q(\mathbf{v} \times \mathbf{B})$. Only the term that includes the magnetic field $q(\mathbf{v} \times \mathbf{B})$ will be dealt with for this article. The independent parameters we use are (i) the momenta of the particles, (ii) the charge (rather, the types) of particles, either positive or negative, and (iii) the current passing through the dipole generating the electromagnetic field. We then measure the angle by which particles get deflected while varying these three parameters and derive an empirical relationship between them.

Keywords: CERN; BL4S; electromagnetism; Lorentz force; deflection; high-energy.

1. Introduction — From the Support Scientists

Beamline for Schools (BL4S) is a yearly international competition, organized by CERN since 2014. Every year between 150 and 200 teams of high school students participate in BL4S. The students have freedom to pursue any scientific question, given the requirement that the experiment must be performed at a given beamline with all the associated constraints. As a result, the proposals range in a wide variety of topics, from experiments testing fundamental questions in particle physics up to tests on detector performance and development. Some of the proposals invariably mimic experiments already present in the literature and which have been performed previously by professional scientists. This is not a detrimental fact since the students will have to learn all the details of the experiment as well as all of the challenges in actually performing the experiment itself, a very challenging (and instructive) task for the students.

Out of all the proposals received, every year, two winning teams are chosen through a competitive process mirroring the usual selection faced by researchers to require “beam time” all over the world. The proposals are evaluated not only on the basis of how feasible the experiment is, but also on how well the students demonstrate their understanding, of the experiment and of the scientific process, as well as their creativity. The two winning teams are then invited to perform their experiments at CERN.

In 2018 one of the winning teams was the “Cryptic Ontics”, from India. Their driving concept was whether cosmic muons could be used to study anomalies in the earth’s magnetic field. This requires knowing well how charged particles and magnetic fields interact. In effect, the experiment broke down into measuring the deflection of relativistic charged particles in a magnetic field and verifying the known properties of the Lorentz force. While the Lorentz force is well established in the physics community, it should not be taken as dogma and can be further studied. The students tackled this with a well thought-out and careful scientific approach.

The Cryptic Ontics’ proposal stood out for the student’s meticulous approach, with a well-defined motivation, which was further distilled into its essence, translating into an experimental setup

targeted to their research question and in line with the beamline capabilities and available detectors. These characteristics, with added value from their very creative video (part of the proposal process), lead to the choice of the Cryptic Ontics as one of the winning teams.

In the process of performing the Cryptic Ontics’ experiment the students had to learn about several different tracking detector technologies, a particular point of focus was the calibration of these detectors. The data of these detectors then had to be combined in order to obtain tracks and with these tracks the deflection angles of the particles could be determined. Given the plethora of particles provided by the CERN beamline, the scope of the experiment was slightly increased: the deflection of different types of charged particles was also measured, while the measurement with only muons was made more challenging, since it was not possible to uniquely identify the muons among this plethora of particles so the young researchers had to execute their measurement with a so-called “high radiation background”, as it is in real experiments. They had indeed to find a way to discriminate the data related to muons from data coming from other particles.

The students were thus confronted with the reality of actually performing an experiment in a beamline and had to adapt and adjust their experimental setup to the available conditions.

2. Introduction — From the Team

The primary aspect of everything that is connected to CERN is scientific but the experience that all of us cherish contains elements of our journey which are not only scientific, but also how we perceive ourselves and our lives there. We were able to make this journey due in part to a combination of fortuitous factors: BL4S’ website being floated over to us by a mentor; the desire to, at the very least, participate, spreading infectiously; and finally, the drafting of a coherent proposal which miraculously (to us, at least) made us win. This narrative forms a significant part of the beloved time we spent working on this project, a project that has given us a great deal of insight into the inner workings of the life of a scientist.

When we got to know that we had won, disbelief washed over us, which was soon replaced by excitement that we channelled towards our experiment. Our principal and teachers felt a well-founded

pride at our having been selected, for it was their liberal nature which allowed us to spend so much time, effort and school resources on our proposal. Without their willingness to participate in this manner of their own, we would never have made it.

2.1. Before the beam

We were all on vacation and our eyes were peeled in search of scientific endeavours when our mentor, Shyam Wuppuluri, first brought to our notice the existence of CERN's Beamline for Schools competition.

Quickly, we formed a team to begin brainstorming, despite not really expecting to win. It was more about the journey than the destination. We began at the only place we knew: *Our school textbooks*. We debated on how good an idea it would be to submit Young's classic Double Slit Experiment or a modification of it and subsequently trawled through the internet of as-yet unperformed thought-experiments proposed by scientists, all of which we felt a deep desire to see performed. We, however, found that we had nowhere near the expertise required to execute experiments such as Popper's experiment¹ or Roger Penrose's FELIX,² both of which had, at a certain point of time, been considered. For a long time, ideas were flung back and forth before we finally settled on the proposal that we sent. We had just been studying classical electromagnetism at that time in school, and so our thoughts were heavily inclined in that direction. Charged particles and the Earth's magnetic field occupied much of the discussions, and it finally crystallized into our initial proposal: To measure the deflection of a certain class of particles under a uniform magnetic field, and compare this with the known deflections of the same under the Earth's magnetic field.

We had decided to use an electromagnetic field to study and observe the behavior of muons. Now, we know that the cosmic rays hitting the Earth's atmosphere produce secondary particles that includes pions which further decay into muons. The trajectories of these muons as they travel down from there is known data. Furthermore, in our experiment, this same class of particles were subjected and observed under a uniform electromagnetic field. Thus, from our experiment our intention was to try and extrapolate possible anomalies in the earth's magnetic field.

2.2. Beam me up! — Getting ready

When the good news came in that we were one of the winners of the competition, our disbelief was surpassed only by our excitement. However, to believe that one can, after travelling to CERN, immediately enter the experimental zone and begin observations is a naive mis-perception.

Safety training itself took up one full day, a day in which the importance of following protocol for our personal safety was impressed upon us. We were given a class on cryogenic safety, a simulation of an emergency situation in the LHC and a lesson on how to operate fire extinguishers, subsequently we had to take online tests on computer security, radiation safety, and so on. This is something we still fondly tease each other about. We had to take multiple tests in order to pass the standards required for being eligible to get our own dosimeters, which measures the radiation dosage received by a person and is very integral in ensuring safety in experimentation. While a few of us passed with flying colors, the others took it a tad too lightly and failed it before being helped by our mentors. The day concluded on a high, with us being handed over our safety shoes and helmets by the jolly Nelson Almeida, giving us reason to enjoy not just the beam days at CERN but also the many secondary activities that we had to perform.

We toured around Geneva, visited the Globe, were taken to the synchrocyclotron, the first particle accelerator put together, and shown an awe-inspiring 3D visualization of how it was constructed and how it functioned; were shown the antimatter factory and allowed to marvel at the mind-blowing complexity of all the detectors and accelerators that there were in it. Indeed, our first taste of real experimentation did not come from our designated experimental area. It came from the S'Cool lab cloud chamber workshop held by Sonia Natale. She began by teaching us about lab etiquette and then moved on to teaching us how to build — you guessed it — a cloud chamber by ourselves. A cloud chamber is basically a particle detector used for visualizing the passage of ionizing radiation and typically consists of a sealed environment containing a supersaturated vapor of water or alcohol. Once we had made it, we were able to view the trajectories of the cosmic rays which keep intermittently bombarding our planet! We were in awe of having created something

that would let us see the particles without any fancy equipment.

2.3. Early beam days

The beginning of our experiment was marked by us placing bets amongst each other regarding how long it would take for us to conduct our experiment satisfactorily: An hour or two? *What could possibly prolong it to nearly two weeks?*, we wondered. We all knew, in theory, of the difference between theory and practice. This difference is governed by the benignly recursive Hofstadter’s Law: it always takes a little longer than you expect, even when you take into account Hofstadter’s Law. All we knew about the Lorentz equation,³ were only from our textbooks.

Even after we entered the experimental area, things were far from smooth sailing. It is generally known that experimentation requires a lot more improvisation than one expects while theorizing, and we discovered this fact firsthand repeatedly over the next few days. But our near-mishaps and close calls are stories for another time.

The members of our team who were assigned the critical job of data analysis, along with our support scientists, worked impressively hard trying to figure out how to calibrate the detectors, learning a lot through example Python scripts provided to us, they tested out the runs, discovered anomalies in the graphs and worked day and night to ensure that we were acquiring the correct data. We would sometimes crash the computers and would have to reset the machines to start over again. However, our mentors helped us work efficiently by changing the commands such that a politely-worded alert would pop-up every time we typed something

wrong! Eventually though, we got everything set up, and were ready to begin our formal analysis!

3. Experimental Setup

Our experimental setup (as seen in Fig. 1) was quite straightforward. It consisted of tracking detectors i.e. the Delay Wire Chambers (DWCs) and the MicroMegas (MMs), to find out where the particles hit, and thus reconstruct its trajectory, a pair of scintillators, or timing detectors^{4,5} that allowed for the speed of the particle to be measured, and an electromagnet producing a uniform magnetic field. Note that the axes are defined as: x upwards in the plane, y directed outside the plane, and z is along the line of the beam.

3.1. T9 beamline characteristics

The BL4S experiments took place in a beamline called the T9⁴ at CERN’s Proton Synchrotron (PS). Protons with a momentum of $\approx 24 \text{ GeVc}^{-1}$ from the PS hit a target called the *North Target* or *Production Target*, generating particles, a stream of which is called the *secondary beam*. In the experimental area, the beam would contain either positively or negatively charged particles with a well-defined momentum, from 0.75 to 10 GeVc^{-1} . The beam consisted of protons, electrons, kaons and pions, and their anti-particle counterparts. Neutral particles such as photons and neutrons are not present.

3.2. Trackers

The delay-wire chambers^{4,6} (DWCs) are tracking detectors which can give the x and y positions of where a particle hit it (*hit positions*).

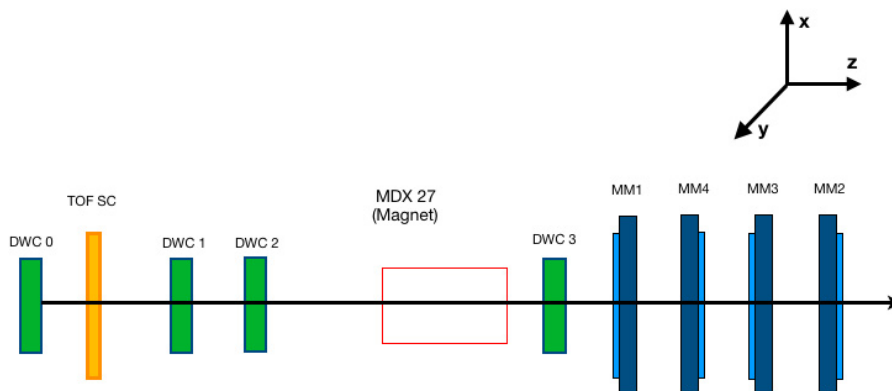


Fig. 1. Diagrammatic representation of Cryptic Ontic’s Beamline For Schools (BL4S) setup at the T9 experimental area (not to scale). TOF0 (the first scintillator) is not shown above as it is placed quite further upstream, outside the experimental area.

The Micromegas^{4,7} (MMs) were slightly different, and could only supply the hit-position in one axis. Thus, simply, one could use two Micromegas placed orthogonal to each other to reconstruct the hit positions in two axes. In our case, they were aligned to the x and y axes. In both sets of detectors, the z -axis coordinates were set as the distance of the detector face from DWC0, which were measured beforehand. Collectively, the DWCs and Micromegas are called *trackers*.

3.3. MDX27 magnet

The MDX27 is an electromagnet of which we could control the amount of input electricity in terms of current, having a range of ≈ 0 A to ≈ 240 A, roughly equivalent to ≈ 0 T to ≈ 1 T. We substituted the strength of the field in terms of *bending power*, where $\beta = B \cdot l$ during analysis. The magnet was used to create a uniform magnetic field to deflect the incoming beam of charged particles. More on the way we used the magnet is mentioned in later sections.

3.4. TOF scintillators

In order to measure the speed of incoming particles, we used a pair of instruments called scintillators,^{4,5} which had a low time resolution $\approx O(1)$ ns. The Time-Of-Flight (TOF) was the difference between the times the scintillators registered a hit. Only one scintillator was placed within our experimental area, as the other was placed roughly 17 meters upstream DWC0.

3.5. Runs

What we will be calling a *run* is essentially a time period wherein a set of particles hit our detectors. The particles hit more or less one at a time, but at a high frequency, so each particle's unique track can be determined. Each run had a set of parameters (called *run conditions*), in particular, charge of the particles, momentum for the beam and amperage of the magnet. While determining the results, we took into account multiple runs to sample particles of varied parameters. Thus, we could reconstruct particle tracks over several runs, and find relations between the angle that the particle gets deflected and the aforementioned variables. This was our eventual goal — to find an overall set of criteria for particle deflection.

4. Analysis

In such a field as high-energy physics, the data must complement the theory. Thus, a vital piece of equipment for us was computer programs. At BL4S, the data acquisition system was borrowed from the ATLAS Experiment across the street, and the data itself was stored and parsed by CERN's own Root framework.⁸ We decided to use Root in C++, as a few of us were already well-versed with the language, but it should be noted that Root has a Python module as well,⁹ and was offered to us for use instead of C++.

4.1. Overview

C++ is an object-oriented language, with which classes can be used in some sense to model “real-world” objects which have attributes and functions. We used this to our advantage, and created several classes, including a *Beam* class, classes for *Magnets* and *Detectors*, and one for *Particles*, which could model any of the particles we wished to work with. Properties were inherited appropriately between classes. A *Run* class was also created, where run conditions were specified for *Run* instances, such as the momentum and amperage. The purpose of this was to create a custom database system, that could find runs with specific properties, either in terms of the run conditions, or additional parameters such as maximum particles, and then load the necessary file(s). The relationships between these classes are described in Fig. 2. Root facilitated the appropriate graphing classes, which were quite easy to implement.

With the code in place, the actual *analysis* had a number of steps, each as important as the next. The process of the analysis is described in detail below:

4.1.1. Calibration

As a very important first step, all detectors were calibrated. This meant carrying out procedures that gave us information about each detector's unique “calibration constants”, used in the reconstruction process. The positional offsets of the trackers with respect to the center of the beam path were also important to note, and were taken into account to accurately reconstruct particle paths. For the pair of TOF scintillators, the offset was the recorded time difference between the hits when both instruments

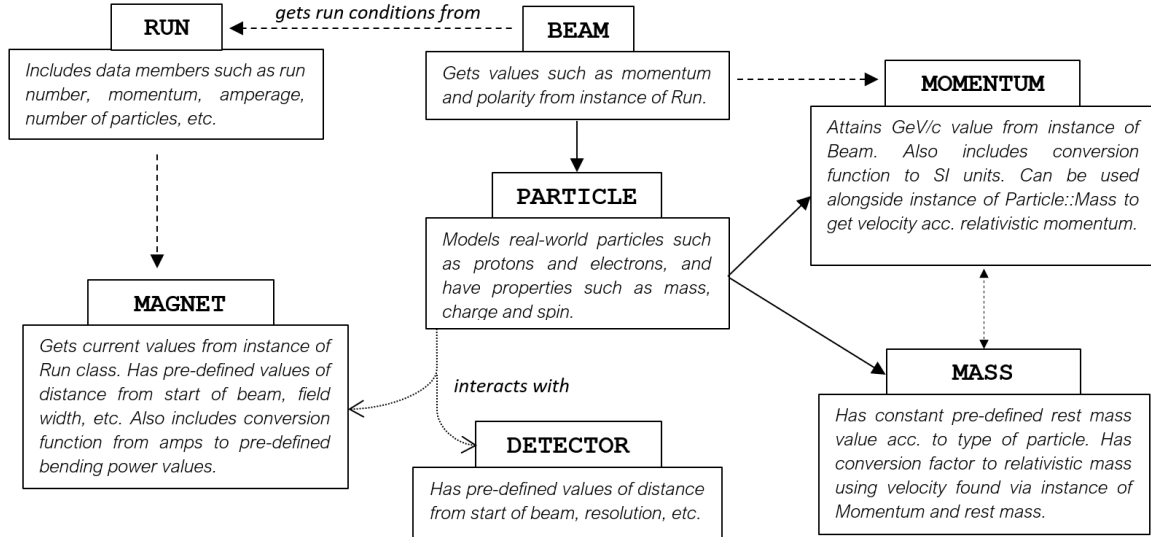


Fig. 2. Selection of custom-defined classes used and the interactions of their instances within the code.

were positioned right next to each other. The magnetic field produced by the magnet when off was noted, due to factors such as magnetic hysteresis,¹⁰ and was taken into account during the analysis.

4.1.2. Reconstruction

The data, which was stored in a `.root` binary file format, was first parsed through some code that calculated the hit-positions on the x and y axes from each of the DWCs and Micromegas respectively (Fig. 3). The z -axis coordinates are pre-defined as the distance of the detector face along the beam path. This can be used to construct the direction of the velocity vectors. Knowing the distance of the TOF scintillators and the time it takes a particle to traverse that distance, one can calculate the speed of the particle via $speed = \Delta distance / \Delta time$. Thus the precise 3D reconstruction of the particle's trajectory can be traced and speed measured.

4.1.3. Graphing

Since we attained the hit-positions in the earlier step, we can now calculate the angle the particle is deflected by the magnetic field. This is simply done by subtracting the initial angle from the final angle that the particle makes, θ . The mean and standard deviation of the angle for each set of runs was calculated and graphed appropriately. These were drawn with Root's TH1D (histograms), and TGraphErrors (graphs with error bars) classes, similar to some of Python's matplotlib functions.

4.1.4. Interpretation

The point on the graphs were *fit* with appropriate curves, which then were interpreted as relations. The process used to determine these curves is called *regression*.¹¹ More details on regression and how we justified fits are given in Sec. A.1.

4.1.5. Verification

Theoretical formulae for the angle of deflection θ based on the Lorentz force³ were made and curves were drawn for comparison to our experimentally obtained fits. In particular, the formula used was

$$\theta = \sin^{-1} \left(\frac{q\beta}{p} \right)$$

where q is charge, $\beta = B \cdot l$ is bending power and p is momentum. It is important to note that the magnetic field produced by the electromagnet was not a perfectly uniform one, but the above formula is applicable for a uniform field in a volume with a given length l . The values for β used were the effective bending powers of the electromagnet, thus we continued by treating it as if it did have a uniform field.

For all the applicable graphs, the red fit curve is our experimental analysis, and the green curve is the expected theoretical relation.

4.2. Finding correlations

Our idea relied on finding the relation between how far the particle gets deflected laterally versus the

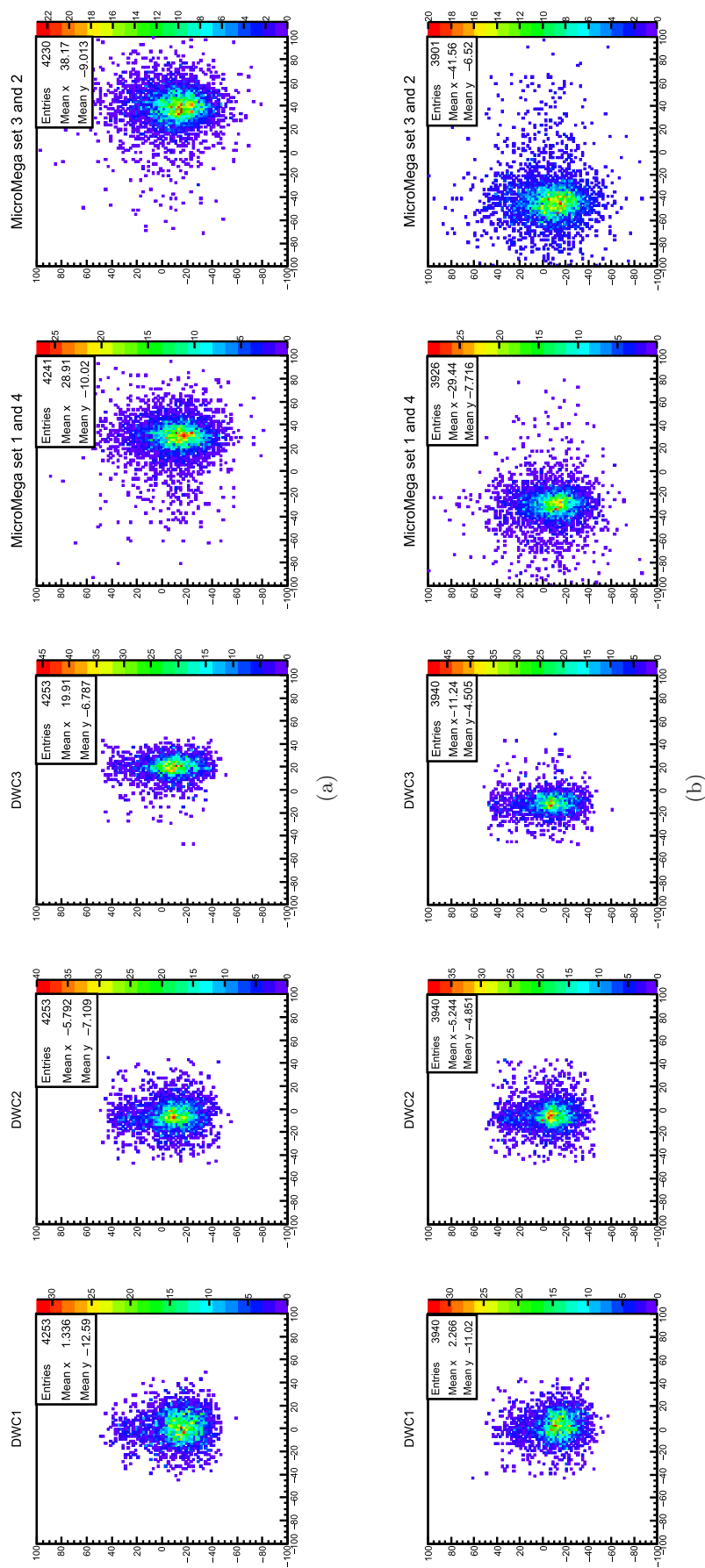


Fig. 3. Examples of the reconstruction of the hit positions on various detectors over time. x and y axes are measured in mm . (a) This run reconstructs hit positions for a positive run as 2D Histograms, showing particles deflecting to the right side, according to convention and (b) the second reconstruction has the same run conditions as the one above, but oppositely charged particles.

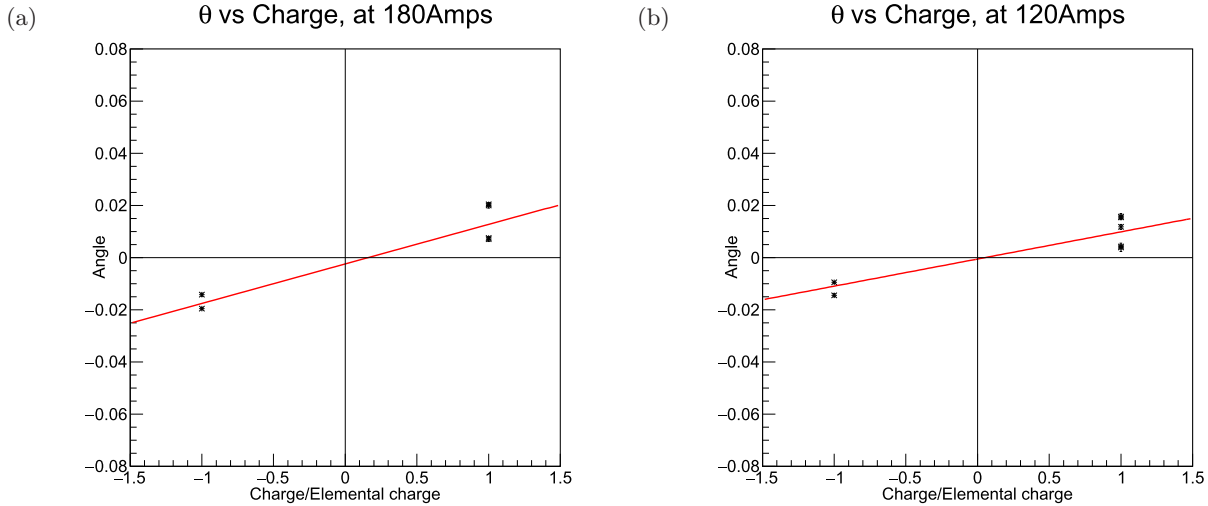


Fig. 4. θ versus *Charge* for a set of runs. As can be interpreted, positively charged particles tend to show a positive deviation, and similar properties can be seen for negative runs. The x -axis shows the particle's charge in units of fundamental charge e . (a) Set of runs at 180 A ($\beta \approx 0.40373$) and (b) set of runs at 120 A ($\beta \approx 0.27025$).

parameters we could change, i.e. charge (q), momentum (p), and magnetic field (B) (viz. bending power β), and then find out how exactly they interact.

4.2.1. Charge

The T9 Beamline could provide to us either a *positive* or *negative* beam.⁴ This meant that the incoming beam could provide a beam of positive particles, such as protons and positrons, or negative particles, like negative pions and electrons. Both types comprised of singly charged particles. We see graphically, that positive particles and negative particles get pushed in opposite directions (e.g. Fig. 4).

Thus, we can conclude:

$$\theta \propto q. \quad (1)$$

In simple terms, oppositely charged beams deflected in opposite directions when all other properties remained the same.

4.2.2. Momentum

The T9 Beamline supplied to us various beam momenta, and it was suggested to us to use a variety, ranging from 3.5 GeVc^{-1} to 10 GeVc^{-1} for both positive and negative beams.⁴ Thus, by varying the momentum over several runs, a sample of results are given in Fig. 5.

Thus we may conclude that:

$$\theta \propto \frac{1}{p}. \quad (2)$$

Classically speaking, one might wish to calculate velocity using $\mathbf{p} = m\mathbf{v}$, and gain a relationship between θ and \mathbf{v} . However, we are using particles moving close to the speed of light, thus relativity ensures the relationship between \mathbf{p} and \mathbf{v} is a little more complex. The direction of both however, remain the same. (More on this can be found in Sec. A.3.)

4.2.3. Bending power

The magnetic field was supplied by the electromagnet MDX27, which was controlled through the amount of current passed through it, from ≈ 0 to $\approx 240 \text{ A}$, which corresponds to roughly ≈ 0 to $\approx 1 \text{ T}$. Due to factors such as the small imperfections produced in the magnetic field and the bulging of the field around the edges of the magnet itself, the actual properties of the field could not be accurately calculated. Thus we were handed bending power values β which were measured by engineers prior to our experiment. This could be substituted for $B \cdot l$, i.e. field strength times length of the field. This was a useful substitution for us, and variance in β does correspond to a proportional variance in field strength (e.g. Fig. 6). Thus we can conclude that

$$\theta \propto \beta \quad (\because \theta \propto |\mathbf{B}|). \quad (3)$$

Put simply, the stronger the bending power or magnetic field, the greater is the deflection, and hence the force.

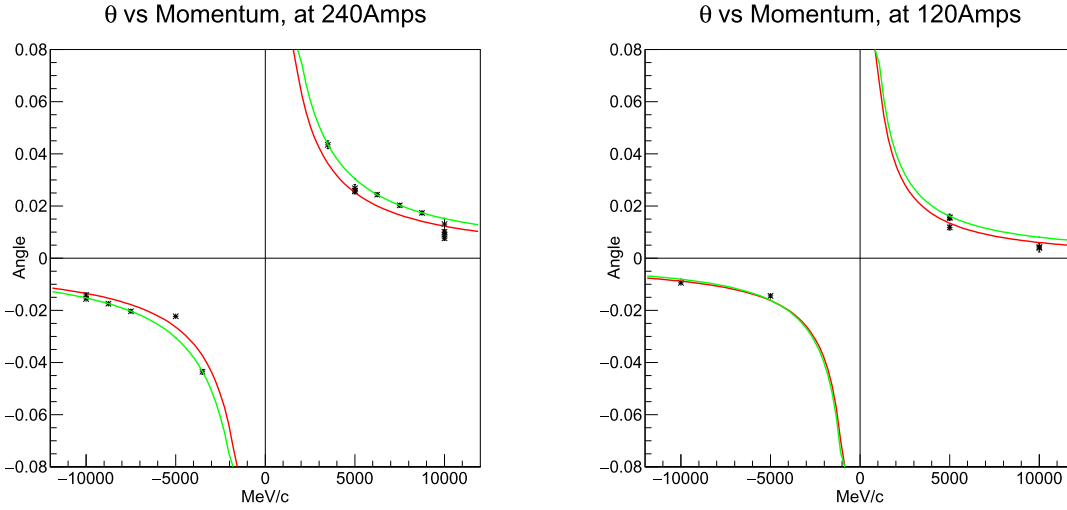


Fig. 5. For a particular set amperage, θ versus momentum follows a $1/x$ shaped curve. Note that a *negative* momentum just implies the particles carry negative charge.

4.2.4. Cross product

It has been previously established experimentally that the force applied on a moving charged body is perpendicular to the direction of the magnetic field.¹² Thus, in our setup, we move forward with this idea, and assume that there must be a cross-product between \mathbf{v} and \mathbf{B} . In this section, the process used to experimentally verify this assumption is discussed.

In order to verify our assumption of the cross-product nature of force \mathbf{F} in terms of \mathbf{v} and \mathbf{B} , we can check the accelerations in each axis to see if they correspond to the theoretical accelerations (e.g. Fig. 7). The way we did this, in terms of analysis,

is to consider the paths before and after the magnetic field as vectors. We can then measure the change in velocities, the acceleration, in each axis.

The magnitude of velocity can be calculated using the TOF scintillators. We can thus figure out the approximate time that it is accelerating in the magnetic field:

$$t = \frac{l}{|\mathbf{v}| \cos\left(\frac{\theta}{2}\right)}$$

where $l \approx$ width of magnetic field and find out the average acceleration in each axis by simply implementing $a = v/t$.

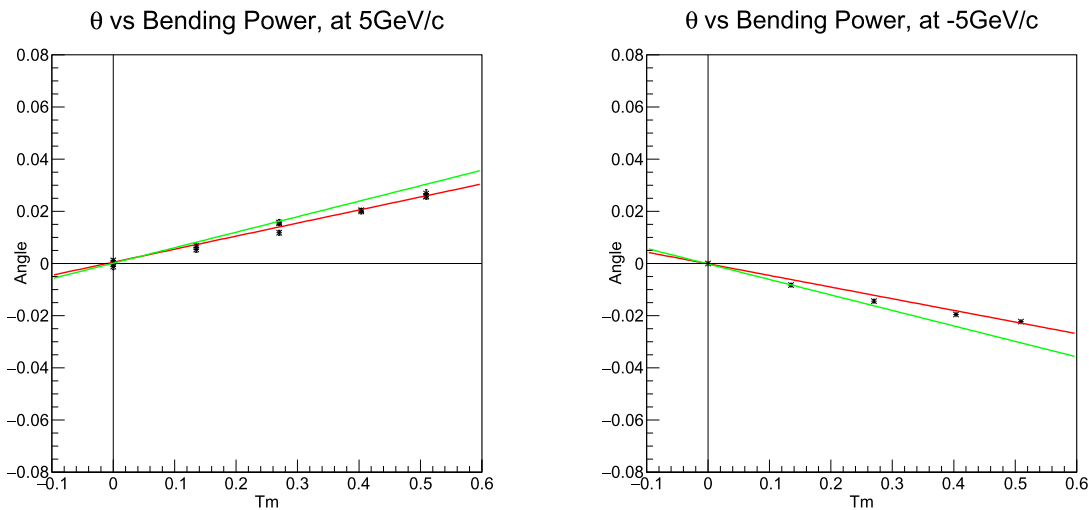


Fig. 6. Given a set momentum, θ shows a direct variance with respect to β , shown here. Bending power is given in units of Tesla-meter. We can conclude that θ , by extension is also directly proportional to the strength of the magnetic field $|\mathbf{B}|$.

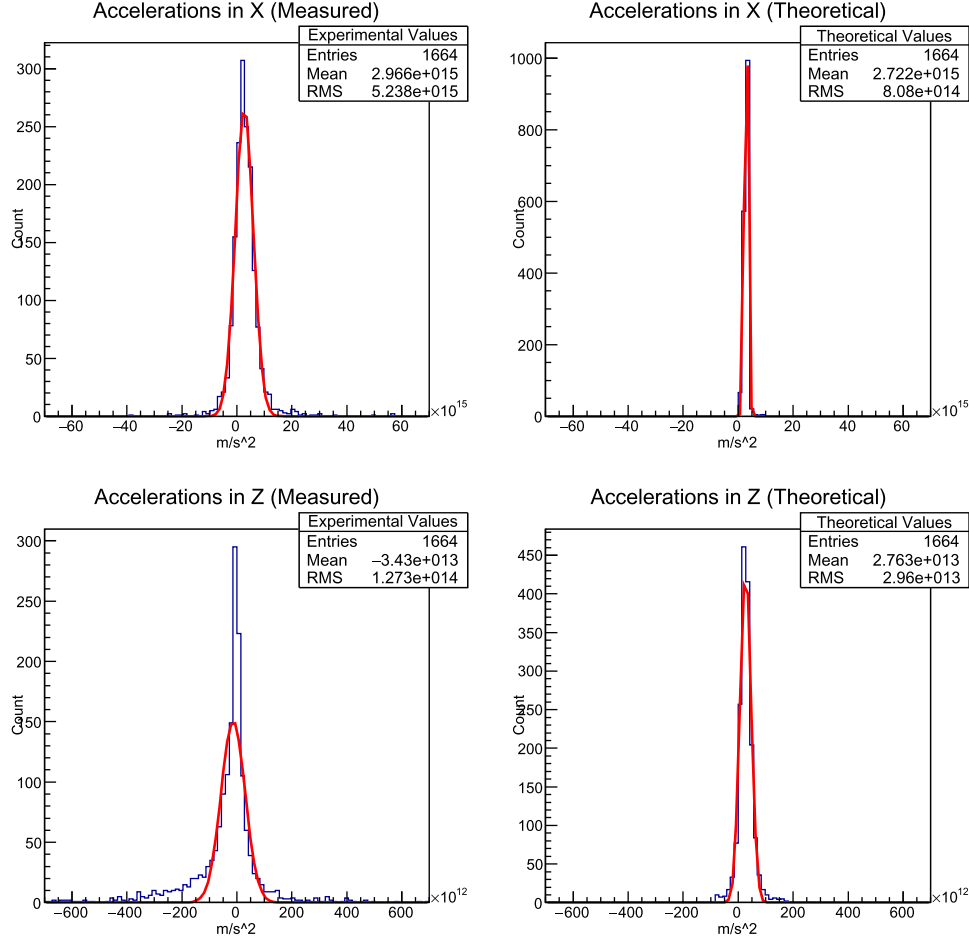


Fig. 7. Comparison of x -axis and z -axis component acceleration. This particular run is of 8.75 GeVc^{-1} , and with an amperage of 240 A i.e. $\beta \approx 0.5095 \text{ Tm}$. The means of the experimentally and theoretically calculated accelerations are quite similar for the x -axis. Note that the theoretical calculations do take into account the initial velocity vector that each particle takes, and as such carries over some amount of experimental error and uncertainty. The y -axis is not shown as acceleration is expected only in the x - and z -axes.

Here, we notice that the experimental histograms of our data have a high standard deviation value as opposed to the theoretical ones. This can be because of a few factors, most prominently scattering of particles in the air and the precision of our instruments. Thus, it may or may not be reasonably expected that with more data, one would get a more confident result. Additionally, the z -axis accelerations seem to be incongruous with theoretic calculations at first, but are well within experimental uncertainties (refer to Sec. A.4). For more on how the theoretical and experimental acceleration values were reached, please see Sec. A.5.

4.2.5. Results

From the analysis we get the following relations:

(1) $\theta \propto q$

(2) $\theta \propto \beta$

(3) $\theta \propto \frac{1}{p}$

(4) The force acts perpendicular to both \mathbf{v} and \mathbf{B} .

Note: We have made an idealization here for the sake of simplicity, namely, that the particle is entirely aligned along the z -axis.

5. Concluding Derivation

In the previous sections, we have already established how θ varies with respect to q , β and p . We can combine these as follows:

$$\theta = \frac{Kq\beta}{p}$$

where K is an arbitrary constant of proportionality, which can be determined experimentally by

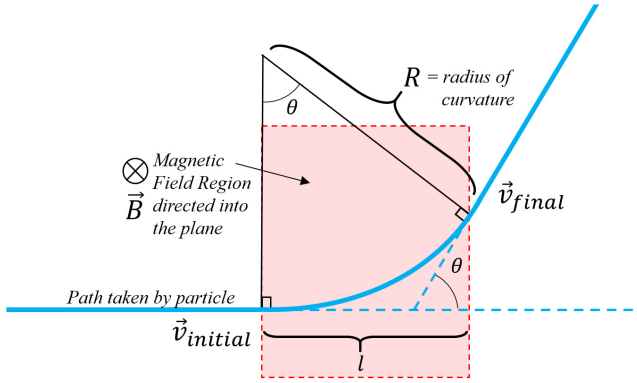


Fig. 8. Deflection of particle inside the magnetic field.

substituting the values of q , β , θ and p . Figure 8 describes graphically the variables used in the following derivation.

We know that

$$\lim_{x \rightarrow 0} \sin(x) = x.$$

The experimental angles are in the range of 0° to 5° , thus the simple approximation of $\theta \approx \sin(\theta)$, can be used.

Also

$$\sin(\theta) = \frac{l}{R}.$$

Equating the two,

$$\frac{l}{R} = \frac{Kq\beta}{p}.$$

Substituting $\beta = B \cdot l$,

$$\begin{aligned} \frac{1}{R} &= \frac{KqB}{p} \\ \therefore \frac{p}{R} &= KqB. \end{aligned}$$

Substituting $p = \gamma mv$,

$$\frac{\gamma mv}{R} = KqB. \tag{4}$$

Multiplying v on both sides,

$$\begin{aligned} \frac{\gamma mv^2}{R} &= KqvB \\ \therefore F &= KqvB \end{aligned}$$

where F is the centripetal force acting on the particle due to the magnetic field. Experimentally K was deduced to be 1 (as described in Sec. A.7). Therefore, F was found to be:

$$F = qvB.$$

In terms of direction, we see that $\hat{p} = \hat{v}$. Thus the product between \mathbf{v} and \mathbf{B} is a cross-product, as the resultant is a vector that is orthogonal to both — a characteristic of cross-products. Thus, in conclusion:

$$\mathbf{F} = q(\mathbf{v} \times \mathbf{B}).$$

6. Discussion

Our initial idea was inspired from a flavor of Gauge system's theory first formulated by Hermann Weyl. The idea of Weyl concerns with the very aspect of measurement which is quite central to physics. Measurement is the comparison of two different attributes, say two different lengths and Weyl suggests that when two such lengths have to be compared, the result may depend on the route pursued in passing from one place to the other. This may perhaps be due to the effect of gravitational and various other fields that are present along the path.

The general features of these field theories is that though these fundamental fields themselves cannot be measured, we can measure the associated attributes and infer something about the fields, in general.

But rather typically, as mentioned before, theory rarely converts itself smoothly into experiment. We had wished to isolate muons from the other host of particles it would be arriving with. However, when we placed filters in order to allow only the muons to pass (said filters being nothing but large iron blocks, for muons are known to have a high penetration power through solids), we found that they were being scattered to a very large extent due to these very filters. This made it difficult for us to study and quantify their behavior. We were thus led onto our current line of thought: a top-down reconstruction of the mathematical equation describing the behavior of charged particles under the influence of a uniform magnetic field.

A striking fact comes to light when we carefully examine our reconstructive analysis: All the empirical consequences of the Lorentz force can be made explicit in terms of charge, velocity and current. Within the context of our setup, future predictions can be purely made on the relations derived. We are now in a position to put forward the following question:

- Why does one need to posit an intermediate quantity known as the "Magnetic field" and substitute it into the Lorentz force equation?

This leads us to the immediate conclusion that the physical quantity known as the magnetic field must necessarily have been discovered in a manner that had nothing to do with moving charges and electricity; and indeed, that is the case, for the phenomena of magnetism that was first discovered via certain special rocks, in the complete absence of an artificially applied flow of electrons. It hints at the fact that it is — empirically speaking, at least — wholly dispensable with for any flavor electromagnetic analysis which is based on the Lorentz force equation, and most definitely with predictions within our experimental setup.

The late physicist Murray Gell-Mann while giving a talk on the *beauty of physics* remarked: *Three principles — the conformability of nature to herself, the applicability of the criterion of simplicity, and the “unreasonable effectiveness” of certain parts of mathematics in describing physical reality — are thus consequences of the underlying law of the elementary particles and their interactions. Those three principles need not be assumed as separate metaphysical postulates. Instead, they are emergent properties of the fundamental laws of physics.*¹³

Over the countless hours of concentrated effort, our objective was to provide a visible connection between these three principles and how using basic laws of physics combined with some simple and yet elegant mathematics ties into our observation of nature so perfectly, further revealing how the fundamental relationship of electricity and magnetism, like the end of a maze, remains one — but the paths leading to it can be *electrically* different.

7. Going Forward

Our time at CERN provided us with new insights and skills that we could never have attained otherwise, whether it was learning how to maneuver around all the physical and mental blocks while solving real-world problems, to being able to help one another in inter-disciplinary ways, from coding to culture, from physics to public speaking, from engineering to education. When we returned, we made sure to spread awareness about STEM research in our school and others, and took hands-on workshops for middle and high school students, eager to soak up as much learning as they could.

Our team members have gone on to study in universities such as UC Berkeley, UC San Diego, University of Groningen, Lund University and the

Indian Institute for Science Education and Research (Kolkata), primarily in STEM-related fields.

The Beamline for Schools Competition continues to inspire us to take up more projects and competitions ourselves and to also carry the torch forward and initiate conversation about science and collaboration in our local communities.

Acknowledgments

Last but not the least, the Cryptic Optics would like to thank Sarah Aretz and all those wonderful people who have made it possible for us to have this experience, from our guides to our support scientists, as well as all the other staff at CERN, including the non-science and support staff, who added their unique human touch to the experience and helping us *per aspera ad astra*.

We would of course, love to thank our own school’s principal, Ms Avnita Bir, and our mentors who accompanied us, Rajeev Maurya and Shyam Wuppuluri, who have been guiding us and giving us their knowledge both before and after our trip to CERN, as well as the rest of the teaching and non-teaching staff at RN Podar School.

We also give our heartfelt gratitude to our families and friends who helped us mentally, physically, spiritually, and even technically during the course of the project. We would also like to acknowledge James Hirst, who began guiding us even before we arrived at CERN, and finally, the Beamcats, the winning team from the Philippines, for being such pleasant peers and now warm friends.

References

1. K. R. Popper, *Logik der Forschung* (JCB Mohr Tübingen, 1989).
2. R. Penrose, Gravitational collapse of the wave-function: an experimentally testable proposal, in *The Ninth Marcel Grossmann Meeting: On Recent Developments in Theoretical and Experimental General Relativity, Gravitation and Relativistic Field Theories (In 3 Volumes)* (2002).
3. I. S. Grant and W. R. Phillips, *Electromagnetism* (John Wiley & Sons, 2013).
4. Beamline for schools beam and detectors https://beamlineforschools.cern/sites/beamline-for-schools.web.cern.ch/files/BL4S-Beam-and-detectors_2018.pdf (2018).
5. S. C. Curran and J. D. Craggs, *Counting Tubes: Theory and Applications* (Academic Press, 1949).

6. J. Spanggaard, *Delay Wire Chambers — A Users Guide*, Tech. Rep., CERN-SL-Note-98-023-BI (1998).
7. Y. Giomataris, P. Rebourgeard, J. P. Robert and G. Charpak, *Nuclear Instruments and Methods in Physics Research Section A: Accelerators, Spectrometers, Detectors and Associated Equipment* **376**, 29 (1996).
8. R. Brun and F. Rademakers, *Nuclear Instruments and Methods in Physics Research Section A: Accelerators, Spectrometers, Detectors and Associated Equipment* **389**, 81 (1997).
9. S. Witowski, *Python at CERN*, Tech. Rep., CERN (2017).
10. S. Chikazumi and C. D. Graham, *Physics of Ferromagnetism 2e*, International Series of Monographs of Physics, Vol. 94 (Oxford University Press on Demand, 2009).
11. K. Smith, *Biometrika* **12**, 1 (1918).
12. J. J. Thomson, *The London, Edinburgh, and Dublin Philosophical Magazine J. Sci.* **11**, 229 (1881).
13. M. Gell-Mann, Beauty, truth and ... physics? (TED Conferences LLC, March 2007).
14. G. Claeskens and N. L. e. a. Hjort, *Model Selection and Model Averaging* (Cambridge University Press, 2008).
15. M. Tanabashi, K. Hagiwara, K. Hikasa, K. Nakamura, Y. Sumino, F. Takahashi, J. Tanaka, K. Agashe, G. Aielli, C. Amsler *et al.*, *Phys. Rev. D* **98**, 030001 (2018).
16. H. Broomfield, J. Hirst, M. Raven, M. Joos, T. Vafeiadis, T. Chung, J. Harrow, D. Khoo, T. Kwok, J. Li *et al.*, *Phys. Educat.* **53**, 055011 (2018).
17. G. Cramer, *Introduction a l'analyse des lignes courbes algebriques par Gabriel Cramer...* (chez les freres Cramer & Cl. Philibert, 1750).

Appendix A

This section further elaborates on some of the more technical ideas discussed earlier in the article.

A.1. Regression

In theory, any curve can be fit onto any set of data points.¹¹ The error of the fit is calculated according to root-mean-square deviation RMS, or the average distance between the predicted point and the actual value. If you have n unique points as a function of x , you can perfectly fit an $n - 1$ degree polynomial onto it, i.e. with zero error. Think how any two points form a line perfectly. If the real-world relation is actually a linear fit, but you try to fit a

higher degree polynomial, you will technically get a better (lower error) fit, but that may not reflect reality, or offer better predictions for new data. This idea is called *overfitting*.¹⁴

Continuing, if you fit a curve to a set of points, say the points we get from bending power β versus angle of deviation θ , with a higher degree polynomial (e.g. a quintic) rather than a linear curve, you will get a valid $ax^5 + bx^4 + cx^3 + dx^2 + ex + f$ fit, depending on how many unique x values you have. However, the values a , b , c , and d will be extremely small, tending to zero for a perfect linear fit, whereas e and f will be much more significant. Thus, practically, you will get a straight line, or a proportional relationship. For a non-polynomial relationship, this can be approximated using the well-known method of Taylor series approximation as described in Sec. A.2.

A.2. Polynomial regression in terms of sin

In reality, β versus θ follow a sinusoidal relation, but if we consider the same principle of regression while trying to fit data with the Taylor series approximation of sine:

$$\sin(x) = x - \frac{x^3}{3!} + \frac{x^5}{5!} - \frac{x^7}{7!} + \dots$$

only the coefficient of the first term will have a significant value, thus approximating to a linear relationship for small values such as attained with our setup. Indeed the error in the fit for a sin or a linear function are very similar. Essentially any function can be approximated using an arbitrary number of terms in an infinite series. In this case, if we just take the first term, we get a relative error of less than 1% for angles under $\approx 14^\circ$ or 0.244 radians. This idea is the basis of what is commonly called the *sin angle approximation for small angles*.

A.3. Relativistic momentum and velocity

With the knowledge of the rest masses of the particles (m) that constituted the beam,¹⁵ we could then calculate the velocity of each using the relation for relativistic momentum. Figure 9 shows the calculated and experimentally determined speeds of two sample runs.

$$p = \gamma mv \tag{A.1}$$

where γ is the Lorentz factor:

$$\frac{1}{\sqrt{1 - \frac{v^2}{c^2}}}$$

Using elementary algebra, one would reach

$$v = \frac{pc}{\sqrt{p^2 + m^2c^2}}$$

Thus v versus p is nonlinear at relativistic speeds. More about relativity can be seen in *Testing the Validity of the Lorentz Factor*¹⁶ an article by a previous winning team of the BL4S competition.

A.4. Acceleration along the z -axis

One might also notice a significant difference between the observed acceleration in z against the theoretical acceleration. But it is imperative to note how the theoretical acceleration is determined. The initial \hat{v}_i (i.e. velocity along the x -axis) is first obtained, using detectors, whose resolution is close to about $450 \mu\text{m}$. Then these positions obtained are converted to unit vectors and are thus dimensionless, and only indicate the inclination of the three vectors to the three axes i.e. x, y, z . After the unit vector is obtained, it is multiplied with $|\mathbf{v}|$ (or just V), $|\mathbf{B}|$ (or just B) and q and divided by the m which is the mass of the particle, after which we get values

$O(10^{13}) \text{ms}^{-2}$. The mean theoretical acceleration in z for the particular run was $2.76 \times 10^{13} \text{ms}^{-2}$.

The formula for the theoretical acceleration along the z -axis was:

$$\mathbf{a}_k = \frac{qVB\hat{v}_i}{m}$$

$$\therefore \mathbf{v}_i = \frac{m\mathbf{a}_k}{qVB}$$

We now observe that $\hat{v}_i \approx 10^{-4}$. The resolution of the detectors is around $450 \mu\text{m} = 4.5 \times 10^{-4} \text{m}$. Additionally, there exists an uncertainty in the distances measured between the detectors in the direction of the z -axis. We posit that the inaccuracy stems from these uncertainties. This affects both the x and z axes, but since the acceleration in the x -axis is greater in general, it is less noticeable.

A.5. Examining the product between \mathbf{v} and \mathbf{B}

Previously, we have established a relation between the force acting on a particle and the variables tested in the scope of our experiment. In doing so, we assumed that the force acting on the particle is perpendicular to the initial velocity \mathbf{v}_i and the magnetic field \mathbf{B} . To validate this assumption, the experimental and theoretical values of the acceleration inside the magnetic field were compared.

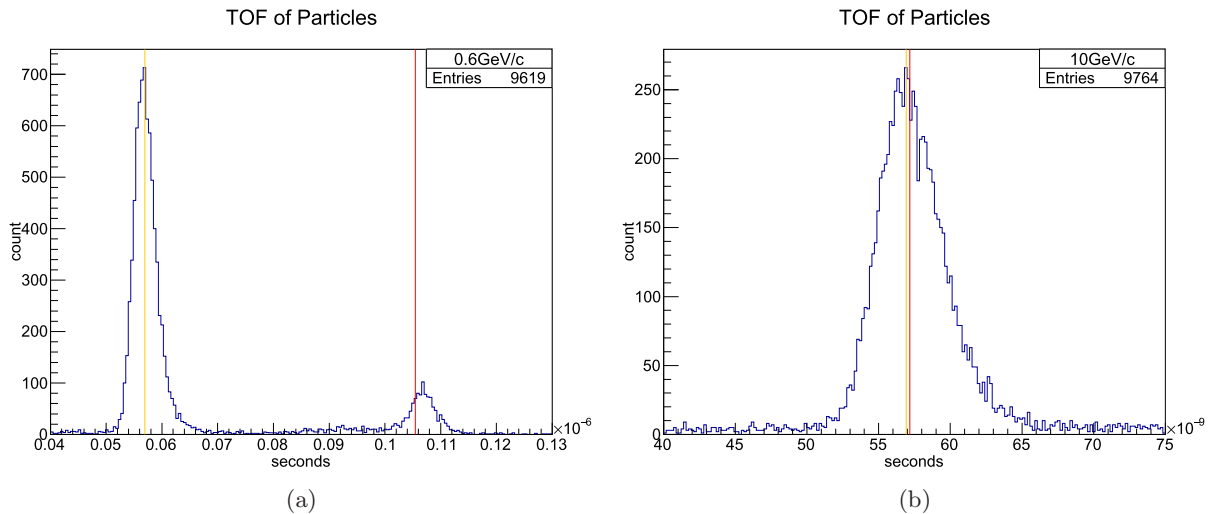


Fig. 9. Examples of TOF reconstructions for two runs. The yellow line indicates calculated positron TOF, and the red line indicates proton TOF, as calculated using special relativity. (a) This run is a 0.6GeVc^{-1} . It is clear that there are two peaks that line up well with the expected and (b) at higher momenta, such as here with 10GeVc^{-1} , it gets harder to discern between particles based on TOF, and the resolution of our scintillator setup is insufficient for such a purpose.

A.5.1. Calculating experimental acceleration

Let us define the initial velocity vector of the particles to be \mathbf{v}_i

$$\mathbf{v}_i = V \cdot \hat{v}_i, \quad \hat{v}_i = \frac{\{a\hat{i} + b\hat{j} + c\hat{k}\}}{\sqrt{a^2 + b^2 + c^2}}$$

where $V = |\mathbf{v}_i|$ and $\{a\hat{i} + b\hat{j} + c\hat{k}\}$ are the unit vectors along three mutually orthogonal axes, i.e. x, y, z . Let us define the final velocity vector of the particles to be \mathbf{v}_f

$$\mathbf{v}_f = V \cdot \hat{v}_f$$

$$\hat{v}_f = \frac{\{e\hat{i} + f\hat{j} + g\hat{k}\}}{\sqrt{e^2 + f^2 + g^2}}$$

It was assumed that the magnitude of the velocity V after acceleration remains the same as before, as when centripetal force is applied, it would not change the overall magnitude, just the direction of velocity. Thus, $|\mathbf{v}_i| = |\mathbf{v}_f| = V$.

We know that:

$$\mathbf{a} = \frac{\Delta \mathbf{v}}{\Delta t}$$

Using this

$$\mathbf{a}_{\text{exp}} = \frac{\mathbf{v}_f - \mathbf{v}_i}{t}$$

where,

$$t = \frac{l}{V \cos\left(\frac{\theta}{2}\right)}$$

Let $\theta/2 = \phi$:

$$\therefore \mathbf{a}_{\text{exp}} = V \cos(\phi) \frac{\mathbf{v}_f - \mathbf{v}_i}{l}$$

$$\mathbf{a}_{\text{exp}} = V \cos(\phi) \left(\frac{V \cdot \hat{v}_f - V \cdot \hat{v}_i}{l} \right)$$

A.5.2. Calculating theoretical acceleration

We have already defined the initial velocity vector \mathbf{v}_i in the previous section.

Let us assume the \mathbf{B} to be:

$$\mathbf{B} = B \cdot \hat{B}$$

$$\hat{B} = \frac{\{e\hat{i} + f\hat{j} + g\hat{k}\}}{\sqrt{e^2 + f^2 + g^2}}$$

where $B =$ magnitude of magnetic field and $\{e\hat{i} + f\hat{j} + g\hat{k}\}$ are the unit vectors along three mutually orthogonal axes, i.e. $x, y,$ and z .

Let us assume the force \mathbf{F} to be:

$$\mathbf{F} = F \cdot \hat{F} \tag{A.2}$$

$$\hat{F} = \frac{\{m\hat{i} + n\hat{j} + o\hat{k}\}}{\sqrt{m^2 + n^2 + o^2}} \tag{A.3}$$

where $F =$ magnitude of force and $\{m\hat{i} + n\hat{j} + o\hat{k}\}$ are the unit vectors along three mutually orthogonal axes, i.e. $x, y,$ and z .

Since, in Sec. 4.2.4, we have shown that $\mathbf{F} \perp \mathbf{v}$ and as hypothesised $\mathbf{F} \perp \mathbf{B}$, their respective dot products with \mathbf{F} will be 0.

$$\hat{F} \cdot \hat{v}_i = 0$$

$$\therefore am + bn + co = 0 \tag{A.4}$$

$$\hat{F} \cdot \hat{B} = 0$$

$$\therefore em + fn + go = 0. \tag{A.5}$$

Equations (A.4) and (A.5) can be solved using a method in linear algebra described in Sec. A.6

$$\therefore \frac{m}{bg - fc} = \frac{-n}{ag - ec} = \frac{o}{af - be} = K'$$

$$\therefore m = K'(bg - fc),$$

$$n = -K'(ag - ec),$$

$$o = K'(af - be).$$

Thus after substituting in Eq. (A.3):

$$\hat{F} = \frac{\{(bg - fc)\hat{i} - (ag - ec)\hat{j} + (af - be)\hat{k}\}}{\sqrt{(bg - fc)^2 + (-(ag - ec))^2 + (af - be)^2}}$$

Substituting in Eq. (A.2),

$$\therefore \mathbf{F} = F \frac{\{(bg - fc)\hat{i} - (ag - ec)\hat{j} + (af - be)\hat{k}\}}{\sqrt{(bg - fc)^2 + (-(ag - ec))^2 + (af - be)^2}}$$

where $F = KqVB$. Force acting upon a particle can also be defined as:

$$\mathbf{F} = m_r \mathbf{a}_{\text{th}}$$

where $m_r =$ relativistic mass of the particle γm_{rest} . Now that we have established a formula for force we can equate it to \mathbf{a}_{th} :

$$\therefore \mathbf{a}_{\text{th}} = k_1 \frac{\{(bg - fc)\hat{i} - (ag - ec)\hat{j} + (af - be)\hat{k}\}}{\sqrt{(bg - fc)^2 + (-(ag - ec))^2 + (af - be)^2}}$$

where $k_1 = KqVB/m_r$.

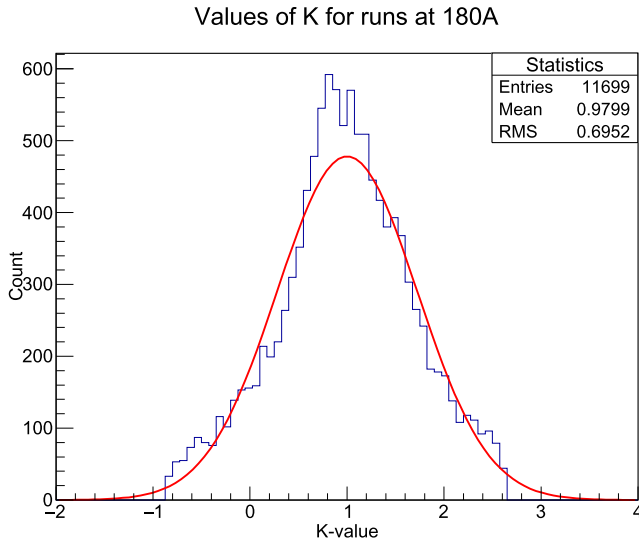


Fig. 10. Experimental values of $K=\theta p/q\beta$ for a selection of runs at 180 amperes.

Experimentally it was observed that along each axis:

$$\mathbf{a}_{\text{th}} = \mathbf{a}_{\text{exp}}.$$

A.6. Linear algebra

Since there are three variables and two equations, Cramer's¹⁷ method of determining the solution for the variables cannot be applied, thus a different approach is required. Consider

$$\begin{bmatrix} a & b & c \\ e & f & g \end{bmatrix} \begin{bmatrix} m \\ n \\ o \end{bmatrix} = \begin{bmatrix} 0 \\ 0 \end{bmatrix}.$$

Let

$$\begin{bmatrix} a & b & c \\ e & f & g \end{bmatrix} = \text{matrix } A.$$

Let

$$\begin{bmatrix} 0 \\ 0 \end{bmatrix} = \text{matrix } B.$$

Since the number of equations is less than the number of variables, there are infinite solutions, but we are only interested in a single one.

Let K' be a constant. On solving the matrix for the solutions we get

$$\frac{m}{bg - fc} = \frac{-n}{ag - ec} = \frac{o}{af - be} = K'$$

$$m = K'(bg - fc)$$

$$n = -K'(ag - ec)$$

$$o = K'(af - be).$$

A.7. Determination of constant K

Using Eq. (4), we know the values of q , β , and p , and experimentally determine θ . We can then rewrite the equation as:

$$K = \frac{\theta p}{q\beta}.$$

For example, for a run with momentum $10 \text{ GeV}c^{-1}$ and bending power 0.5095 (240 amperes), we see a deflection of 0.01865 ± 0.00411 . Inputting this into the above equation gives us a $K = 1.2459 \pm 0.27643$. The values of K attained for several particles for a sample of runs (180 amperes, multiple values of momenta) are shown in Fig. 10. Over several runs, the value of K tends to 1.

Satchit Chatterji is currently studying artificial intelligence, with honours, at the University of Groningen, the Netherlands. He is deeply invested in music and the fine arts. He hopes to understand how human minds work, and to apply AI-inspired problem solving and data analysis techniques to facilitate pure science research, especially in particle physics.

Aayush Desai is currently pursuing physics at Lund University, Sweden. He is an avid basketball player, and has a keen interest in recreational mathematics. He hopes to graduate specializing in theoretical physics.

Aditya Dwarkesh is an undergraduate student pursuing physics at the Indian Institute for Science Education and Research, Kolkata. He was an editor of the TED-Ed newsletter The Eyries and Pyries of Thought writing on analytic philosophy, and was a fourth prize recipient of the Foundational Questions Institute's 2017 essay contest.

Anushree Ganesh is currently pursuing her undergraduate degree in physics at Utrecht University, the Netherlands, and aspires to specialize in theoretical or particle physics at the graduate level.

Ameya Kunder is an undergraduate at the University of California, Berkeley, studying physics and computer science. He wishes to pursue a career in research in the domain of theoretical physics.

Pulkit Malhotra is studying physics and philosophy at the University of California, San Diego. He is currently working with an experimental physics group that uses machine learning to analyze data from CERN's detectors.

Roshni Sahoo is currently studying in the first year of her bachelor's degree in science (physics) at St. Xavier's College, Mumbai. She has been selected for National Initiative on Undergraduate Science 2020 of Homi Bhabha Centre for Science Education (Tata Institute of Fundamental Research).

Jinal Shah has a strong inclination for STEM subjects. She hopes to study physics at university and pursue research further. She is also a passionate artist and enjoys exploring the underlying similarity of art and science.

Kiranbhaskar Velmurugan is currently pursuing a bachelor's degree in computer science engineering at BITS Pilani, Dubai. He is deeply interested in fields like computer science, artificial intelligence, and physics.

Markus Joos studied technical engineering at a university of applied science in Germany. In 1993, he joined CERN where he has focused on the development of software for modular electronics used in data acquisition systems. He is a co-organizer of the ISOTDAQ schools and the technical coordinator of Beamline for Schools.

Cristóvão Beirão Da Cruz E Silva holds a doctorate degree in physics from the "Instituto Superior Técnico" of the University of Lisbon. During his PhD, he worked in the area of experimental particle physics within the CMS collaboration. The work carried out permitted attaining his PhD with distinction in 2016, for his research on the search for the supersymmetric tau partner. In 2018, he started working with the Beamline for Schools (BL4S) competition at CERN as a support scientist. Presently a fellow at CERN, since April 2019, he also has responsibilities in the New Small Wheel detector upgrade for the Atlas detector while continuing his work with the BL4S team.

Gianfranco Morello holds a doctorate degree in physics from the University of Calabria, Italy. In 2018, he assisted the winners of BL4S with the realization of their experiment. Right now he works at INFN in Frascati, Italy.